https://ntrs.nasa.gov/search.jsp?R=20190001926 2019-08-30T22:45:43+00:00Z

Easing into Reality: Experimental Impacts into Slopes and Layers. J.M. Ebel[1], L.E. Dechant[1], J.L.B. Anderson[1], M.J. Cintala[2], and J.B. Plescia[3]. [1]Department of Geoscience, Winona State Univ., Winona, MN 55987. [2]Code XI3, NASA JSC, Houston, TX 77058. [3]Applied Physics Lab, Johns Hopkins University, Laurel, MD 20723. (Corresponding author: JLAnderson@winona.edu)

Introduction: Impact cratering is the dominant geologic process affecting the surfaces of solid bodies throughout our solar system. Because large impacts are (luckily) rare on Earth, the process is studied through experiments, observations of existing structures, numerical modeling, and theory, most of which make the simplifying assumptions that the target is homogeneous, with no substantial topography [1-6].

Craters do not always form on level targets composed of homogeneous loose material. Rather (Fig. 1), they often form on sloped surfaces and in layered targets, both of which significantly influence the excavation and ejecta deposition processes [7,8]. Such craters are common on the Moon and asteroids. We are investigating crater formation in two separate suites of experiments using sloped and layered targets (Fig. 2) at the Experimental Impact Laboratory at NASA Johnson Space Center. An experiment was also performed in a flat, homogenous target to serve as a reference.

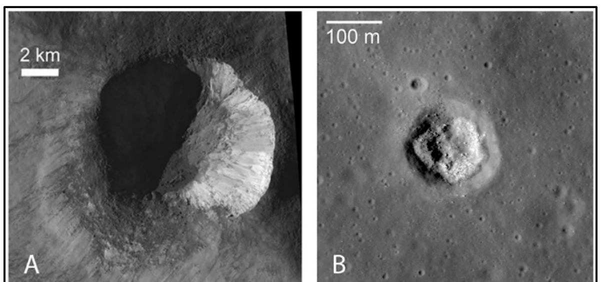

Figure 1. (A) An impact crater formed on the rim of Gibbs crater. Regional slope from top-right to bottom-left is 28°. [-17.50° S/85.18° E] (B) A small impact crater in the lunar mare near the Apollo 12 site showing concentric morphology inferred to be a result of a layer of regolith over a more competent unit. [-3.297° S/336.708° E]

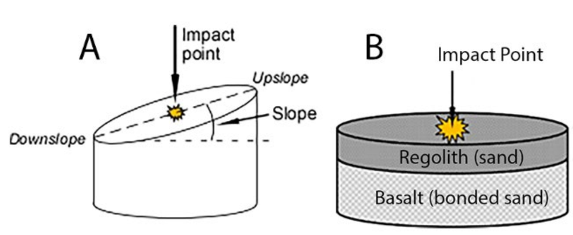

Figure 2. (A) Target design for sloped target experiments. Entire target is filled with loose sand. (B) Target design for layered target experiments. Stronger substrate of bonded sand underlies a thin regolith layer of loose sand.

Experiment Design: Experimental impacts were performed in near-vacuum (< 1 torr), with 3.18-mm aluminum projectiles impacting the target at 1.5 km/s and normal to the floor of the target chamber. The sloped targets consisted of a medium-grained sand (0.4-0.8 mm grain size) and were constructed using sheet-metal templates that, when rolled into a cylinder and inserted into a standard target container, provide a slope of the desired angle (Fig. 2A). The layered targets consisted of the same sand overlying a strong layer of sand that was bonded with sodium silicate ("water-glass") (Fig. 2B). A Next-Engine 3D scanner was used to record the target's configuration before and after each experiment, permitting all post-experiment changes to be referenced to the actual, pre-impact topography. The 3D scans were exported as XYZ files and, using ArcGIS tools, were converted into workable raster datasets. Each experiment was observed with the Ejection-Velocity Measurement System (EVMS) [9] making analysis of ejecta trajectories possible as well.

Sloped Targets: Experiments were conducted with slopes of 5°, 10°, 15°, and 20°; results from the 15° target will be presented here.

The crater on the 15° slope shows little to no rim on the upslope side, rounding of the downslope rim, substantial slumping of the upslope wall, and an offset of the deepest point of the crater downslope from the impact point implying that the regional slope heavily affected the excavation of the growing crater. The topographic maps of the crater on the 15° slope (Fig. 3) and its profile in the downslope direction (Fig. 4) share similarities to those of the lunar crater in Fig. 1A.

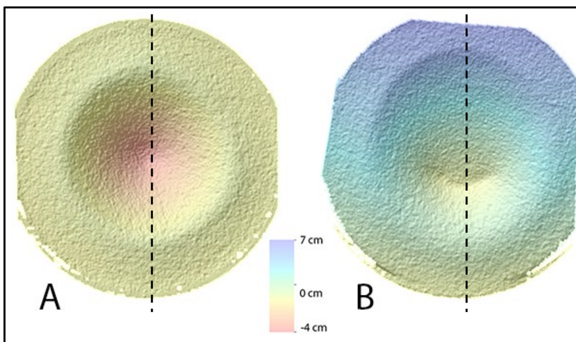

Figure 3. Topographic maps of (A) the reference crater and (B) the crater on the 15° slope. Dashed lines indicate topographic profiles in Figure 4.

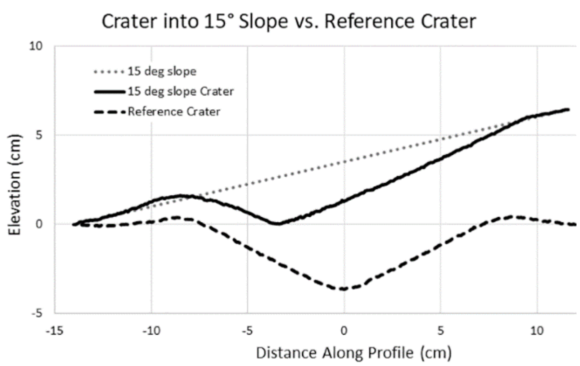

Figure 4. Topographic profiles along the regional slope through the crater on the 15° slope and the reference crater. No vertical exaggeration.

Layered Targets: Our first suite of experiments using strength-layered targets was conducted with approximately 3-, 2-, and 1-cm layers of loose sand "regolith" over the bonded sand. Here we discuss results from the 3-cm regolith target.

At first glance, the final crater in the 3-cm regolith looks just like the reference crater (Fig. 5). It appears very similar in size and shape, with the same cylindrical symmetry. Most importantly, there is no substrate material visible inside the crater and no obvious concentric features in its interior. Even the topographic maps of the two craters (Fig. 6) look nearly identical. There are subtle and important differences, however, that can best be seen in the topographic profiles (Fig. 7). The crater in the 3-cm regolith is both shallower and wider than the reference crater implying that the strength of the subsurface layer affected the cratering flow-field even though no evidence of the stronger unit is visible in the final crater morphology.

Figure 5. Photo of the crater formed into a target with a 3-cm layer of sand over a stronger substrate of bonded sand. The bonded sand is a darker color than the "regolith" sand, as seen in top right corner.

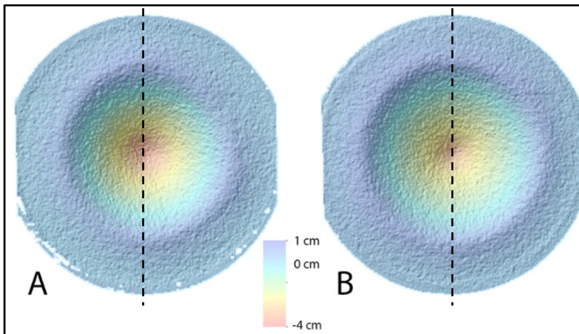

Figure 6. Topographic maps of (A) the reference crater and (B) the crater in the 3-cm regolith target. Note that 6A is the same crater as in Fig. 4A but with a different elevation scale. Dashed lines indicate topographic profiles in Figure 7.

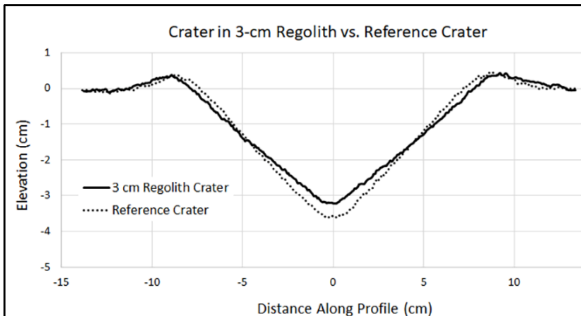

Figure 7. Topographic profiles through the 3-cm regolith and the reference craters. Vertical exaggeration ~2x.

Conclusions: These initial results have implications for the interpretation of planetary craters on slopes and layered targets such as the Moon's maria. With very high-resolution images now the norm, it is important to investigate the effects of regional and even smaller scale slopes and subsurface layers in order to interpret spacecraft observations accurately.

References: [1] Runyon K. & Barnouin O. (2018) Plan.Space.Sci. **160C**. [2] Kenkmann T. et al. (2018) MAPS **53**. [3] Stopar J. et al (2017) Icarus **298**. [4] Bart G. et al. (2011) Icarus **215**. [5] Elbeshausen D. et al. (2013) JGR **118**. [6] Holsapple K. (1993) Ann. Rev. Earth Space Sci. **21**. [7] Quaide, W. & Oberbeck V. (1968) JGR **73**. [8] Plescia J. & Spudis P. (2014) Plan. Space Sci. **103**. [9] Cintala M. et al. (1999) MAPS **34**.

Acknowledgements: This work would not have been possible without EIL gunners Frank Cardenas and Roland Montes and all-around electronics wizard Terry Byers and everything they do to keep things moving forward in the laboratory. Many thanks also to Luke Zwiefelhofer for his insight and efforts in the lab and for tech support at WSU. Fred Calef and Dylan Blumentritt both provided invaluable GIS wisdom. This work is supported by NASA SSW grant NNX16AR92G.